Journal of Marine Science and Technology

Volume 21 | Issue 4 Article 5

DETERMINATION OF MORTAR SATURATION METHODS BASED ON MRI SCANNING IMAGE

Hsiang-Wei Chiang
Department of Harbor and River Engineering, National Taiwan Ocean University, Keelung, Taiwan, R.O.C.

Ran Huang
Department of Harbor and River Engineering, National Taiwan Ocean University, Keelung, Taiwan, R.O.C.,
ranhuang1121@gmail.com

DETERMINATION OF MORTAR SATURATION METHODS BASED ON MRI SCANNING IMAGE

Acknowledgements

The authors wish to express their appreciation to the Preparatory Office of the Institute of Biomedical Sciences (IBMS) for providing the venue and MRI system required for the experiments.

Journal of Marine Science and Technology, Vol. 21, No. 4, pp. 410-416 (2013)
DOI: 10.6119/JMST-012-0522-1

DETERMINATION OF MORTAR SATURATION METHODS BASED ON MRI SCANNING IMAGE

Hsiang-Wei Chiang and Ran Huang

Key words: pore, immersion method, boiling method, vacuum method, MRI.

ABSTRACT

Magnetic resonance imaging (MRI) is widely used in the medical field and among one of the greatest inventions in recent years. In MRI images, the bright zone denotes signals that are generated by water in the specimen. However, solid cement-based materials lack water. Therefore, developing a method to achieve optimal saturation for cement-based materials is crucial for MRI scanning.

In this study, the immersion, boiling, and vacuum methods were used to achieve saturation for various mortar specimens with w/c ratios of 0.45, 0.55, and 0.65. By comparing MRI images and absorption test results, we found that the vacuum method tends to yield satisfactory saturation levels.

I. INTRODUCTION

Concrete is composed of cement, water, coarse aggregate, and fine aggregate. When mixed with water, concrete undergoes a process called hydration that causes it to harden, developing strength. Because of the admixture, hydration, and other physical or chemical factors, concrete contains numerous pores. Regarding the internal structure of concrete, the main concerns are the distribution, size, and type of the pores, and how they are connected. A thorough understanding of pore distribution rules and methods of breaking their links to enhance the durability of concrete would significantly contribute to existing knowledge. According to the reference, ideal pore-measurement technology should have the capabilities to perform the following functions: (1) Measure all concentrated pores, (2) describe the volume, size, shape, and surface of pores, (3) perform the functions of pore-measurement technology without altering the nature or physical structure of the material, (4) precisely measure pores in the research range under the same conditions, (5) allow pore-measurement methods to be reversed anytime and anywhere, and (6) clearly describe the differences between pores [9]. Currently, no pore measurement method can fulfill all these functions because each method has unique objectives and limitations [7]. In recent years, numerous researchers, such as Young *et al*. [11], have used magnetic resonance imaging (MRI) to measure the micro defects of cement pastes. MRI has been proven to be capable of spatially resolving crack structures with widths of tens of micrometers. Jafer *et al*. [8] also used MRI for examining concrete, describing MRI as a "complementary tool for imaging cement pastes". Water has two hydrogen atoms that emit MRI detectable signals when activated [6]. The bright zones in the MRI images represent signals generated by water. Therefore, developing a method to achieve optimal saturation for cement-based materials is crucial for MRI scanning.

The development standards and testing methods for cement-based materials are approved by the American Society for Testing and Material (ASTM). Safiuddin and Hearn [10] discussed the three concrete saturation techniques employed in various ASTM standards. The first is cold-water saturation (CWS). The second is boiling-water saturation (BWS). Both these techniques are employed in the reference ASTM C642. The third technique is vacuum saturation (VAS), referenced in ASTM C1202. Presently, MRI scans of cement-based materials lack saturation specifications. Therefore, for this study, we reference the ASTM-specified immersion method (defined as CWS by Safiuddin *et al*.), boiling method (defined as BWS by Safiuddin *et al*.), and vacuum method (defined as VAS by Safiuddin *et al*.) to determine the most satisfactory method for mortars to attain optimal saturation for MRI.

II. THEORY

The immersion method uses the principle of diffusion to allow the water to saturate the specimens. The boiling method involves immersing the specimens in water at room temperature, gradually heating the water to the boiling point. This method enables extrusion of air bubbles and positive pressure, forcing water into the specimen to achieve saturation. The vacuum method involves placing the specimen in an enclosed container and pressurizing the container to 1 mm-hg less than

Paper submitted 11/17/11; revised 03/21/12; accepted 05/22/12. Author for correspondence: Ran Huang (e-mail: ranhuang1121@gmail.com).
Department of Harbor and River Engineering, National Taiwan Ocean University, Keelung, Taiwan, R.O.C.

the outside environment, and then pouring water into the container. As the fluid shifts from a zone of high pressure to a zone of low pressure, water moves into the pores of the specimen. The basic principles of MRI [5] are summarized below. Hydrogen atoms emit signals that are detectable by MRI. Because electrons and protons have an electric charge and also rotate, their behavior is similar to that of a small current loop. As a moving charge generates a magnetic field, electrons and protons act as small magnets with positive and negative poles. This is known as a magnetic dipole.

When no external magnetic field exists, the magnetic dipole of hydrogen nuclei (with only one proton) does not have a specific direction, and the net magnetization (the sum of all the magnetic dipoles) equals zero. When an external magnetic field exists (commonly defined in discussions on MRI as the Z direction; the intensity of the magnetic field is BO, and is known as the main (magnetic) field), the magnetic dipole of hydrogen nuclei can have two directions. One is parallel and in the same direction as the external magnetic field (+Z), and the other is parallel but in the opposite direction of the external magnetic field (–Z). However, hydrogen nuclei in a higher state of energy can be in a direction parallel to but opposite that of the external magnetic field.

The direction of the magnetic dipole is influenced by the following two factors: the size of the external magnetic field and the energy of the atom. When the external magnetic field is stronger, fewer magnetic dipoles can be in a direction parallel to but opposite that of the external magnetic field. Thus, more magnetic dipoles are oriented in the same direction as the external magnetic field. When the +Z and –Z magnetic dipoles cancel each other out, the direction of net magnetization is the same as that of the external magnetic field (+Z). MRI detects and records the excitation and relaxation signals of all hydrogen atoms in one section of the specimen. To understand the structural or functional changes in various zones of the specimen, spatial location signals must be incorporated into the signals. Briefly, this involves slice selection along z, an axis on the X-Y plane (such as the frequency encoding along x) and another axis on the X-Y plane (such as the phase encoding along y). Practical requirements determine the direction used to perform slice selection, frequency encoding, and phase encoding. The techniques used in this study are the concepts of magnetic field gradients and Fourier transforms.

Spin echo is a common pulse sequence that is used when the intensity of a static magnetic field is insufficient. Thus, it is typically employed to image solid materials with low water content. This is because T2 in the solid materials of mortar is relatively short, and the number of hydrogen nuclei is relatively low. These features complicate the achievement of clear images. Thus, single-point imaging (SPI), a phase-encoding pulse sequence, is an appropriate choice. SPI generates a pulse sequence to every point for sample collection. Additionally, it also alters the gradient pattern to gather spatial information. Although the SPI technique typically requires a lengthier imaging time, it yields high-quality images [4].

Table 1. Specimen designation.

Specimen	w/c ratio	Treatment	Standard
I1	0.45	Immersion method	ASTM C642
I2	0.55	Immersion method	ASTM C642
I3	0.65	Immersion method	ASTM C642
B1	0.45	Boiling method	ASTM C642
B2	0.55	Boiling method	ASTM C642
B3	0.65	Boiling method	ASTM C642
V1	0.45	Vacuum method	ASTM C1202
V2	0.55	Vacuum method	ASTM C1202
V3	0.65	Vacuum method	ASTM C1202

Therefore, for this study, we adopted the SPI pulse sequence to obtain MRI images of mortars.

III. EXPERIMENTAL DETAILS

1. Preparation of Test Specimens

Standard sand, cement, and water were mixed to produce mortars with water-to-cement ratios (w/c ratio) of 0.45, 0.55, and 0.65, respectively. Cylindrical mortar specimens 10 mm in diameter were produced for the MRI and absorption test. The designation of the specimens is shown in Table 1. Cube mortar specimens ($51 \times 51 \times 51$ mm) were created to conduct compressive strength tests according to ASTM C109/C109M-11 [1]. The mortars were subsequently wet cured for 91 days and then air dried for 48 h.

2. Pre-Processing Method for the Cement Specimens to Conduct MRI and Calculate Absorption

2.1 The immersion method according to ASTM C642-06 [2] involves soaking the specimens (mortar with w/c ratios of 0.45, 0.55, and 0.65) in water at room temperature for 48 h to ensure that the water enters the specimen pores and until two successive mass values of the surface-dried sample at 24 h show an increase in mass of less than 0.5% of the previous value.

2.2 The boiling method according to ASTM C642-06 involves immersing the specimens in water at room temperature, gradually heating the water to the boiling point, maintaining the boiling state for 5 h, and then allowing the specimen to cool naturally for 19 h. The specimens (mortar with w/c ratios of 0.45, 0.55, and 0.65) are continually immersed in water at room temperature to ensure that the water enters saturates the pores.

2.3 The vacuum method according to ASTM C1202-97 [3] involves placing the specimens in an enclosed container and activating the vacuum pump until the difference between the pressure inside and outside the container reaches 1 torr (1 mmHg) (at this time, compared to the external surroundings, there is 1 mm-hg of negative pressure in the container). The vacuum pump is then switched off. After the specimens (mortar with w/c ratios

Table 2. Absorption results of various w/c ratios under optimal saturation conditions obtained using the immersion method, boiling method, and vacuum method.

Specimen	Absorption
I1	6.28%
I2	8.60%
I3	9.59%
B1	6.39%
B2	8.98%
B2	10.03%
V1	7.02%
V2	9.18%
V3	10.56%

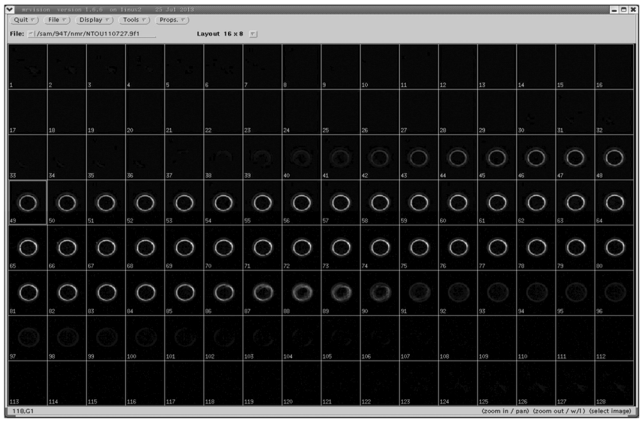

Fig. 1. 128 cross-sectional MRI images of Specimen I1.

of 0.45, 0.55, and 0.65) have been in the container for 3 h, deaerated water is added, and the vacuum pump is activated for a further 1 h. Then, the specimens are allowed to soak in deaerated water for 18 h.

3. MRI

After the absorption tests, MRI experiments were conducted. Mortars with w/c ratios of 0.45, 0.55, and 0.65 were examined separately. This study employed the three saturation methods of immersion, boiling, and vacuum methods were employed. For this study, we used a 9.4 Tasla (8.9 cm in diameter) upright superconducting MRI system. Several parameters must be established before implementing the MRI system; these parameters are outlined below. Repetition time (TR) is the gap in time between the two radio-frequency excitations; the echo delay time (TE) is the time required to receive the echo; the field of view is denoted as FOV; the number of excitations is denoted using NEX; the matrix size refers to the number of signal points obtained from the x-axis, y-axis, and z-axis of the Nx × Ny × Nz image; resolution is the spatial resolution of 1 pixel for the x-axis, y-axis, and z-axis; and scan time is the time required to complete a scan. For this study, the following parameters were set for the MRI system:

TR = 10 ms, TE = 0.026 ms, FOV = 5.0 × 5.0 × 5.0 cm, NEX = 1, matrix size = 128 × 128 × 128, resolution = 391 × 391 × 391 μm, and scan time = 5 h 49 min.

IV. RESULTS AND DISCUSSION

1. Absorption of the Specimen

Eq. (1) is used to calculate the absorption of the specimens

$$\text{Absorption} = (\text{Ws} - \text{Wd})/(\text{Wd}) \times 100\% \quad (1)$$

where, Wd = oven-dry mass of the specimen in air, and Ws = surface-dry mass of the specimen in air (saturated mass after immersion, saturated mass after boiling, saturated mass after vacuum). Table 2 and Fig. 5 show the absorption of the specimens based on the w/c ratios of 0.45, 0.55, and 0.65 obtained using the immersion, boiling, and vacuum methods. When the w/c ratio was 0.45, the absorption achieved using the vacuum method was 7.02%; the absorption achieved using the boiling method was 6.39%; and the absorption achieved using the immersion method was 6.28%. Thus, the vacuum method achieved the highest absorption, the boiling method achieved moderate absorption, and the immersion method achieved the lowest absorption. When the w/c ratios are 0.55 and 0.65, the absorption trends equal that when the w/c ratio is 0.45. Therefore, when the w/c ratios are identical, the absorption obtained using the vacuum method exceeds that obtained using the boiling method. The absorption obtained using the boiling method exceeds that of immersion method. In other words, water cannot completely fill the dead-end pores using the immersion and boiling methods. This result agreed with that reported by Safiuddin and Hearn.

2. MRI

The MRI images with various w/c ratios are top-down images that are overlapped with cross-sectional data divided from the test specimen. Fig. 1 was obtained by evenly separating the specimen I1 into 128 cross-sections identical in height by MRI scanning. The 128 cross-sectional images (Fig. 1) were overlapped to form a top-down image Fig. 2(a) of the water signal distribution in the specimen. The images in Fig. 2(b) and the other figures (Fig. 2(c), 3(a), 3(b), 3(c), 4(a), 4(b), and 4(c)) were obtained using the same procedure. The Figs. 2-4 present MRI images of the specimens and the w/c ratios based on the water absorption and other correlated parameters determined using the three methods. Fig. 2 shows the ratios obtained using the immersion method: Figs. 2(a)-(c) have w/c ratios of 0.45, 0.55, and 0.65, respectively. Fig. 3 shows the ratios obtained using the boiling method: Figs. 3(a)-(c) have w/c ratios of 0.45, 0.55, and 0.65, respectively. Fig. 4 shows the ratios obtained using the vacuum method: Figs. 4(a)-(c) have w/c ratios of 0.45, 0.55, and 0.65, respectively.

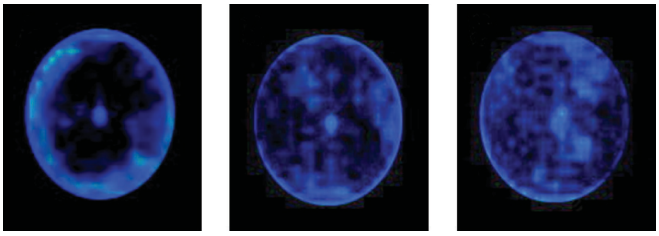

(a) (b) (c)

Fig. 2. MRI images using immersion methods. (a) I1, (b) I2, and (c) I3.

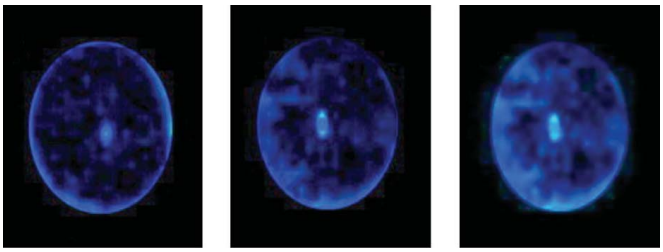

(a) (b) (c)

Fig. 3. MRI images using boiling method. (a) B1, (b) B2, and (c) B3.

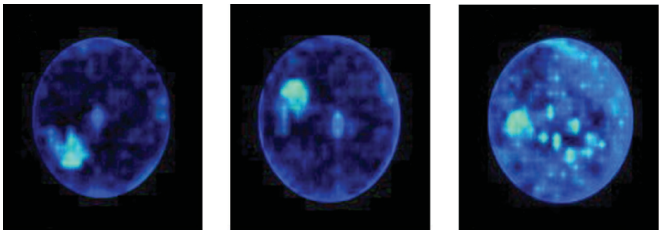

(a) (b) (c)

Fig. 4. MRI images using vacuum method. (a) V1, (b) V2, and (c) V3.

In the MRI images, the bright zones represent signals generated by the water. The locations with signals indicate the presence of water and reveal the location of pores. Regarding the MRI results for the specimens with identical w/c ratios, the vacuum method provided more signals compared to the boiling method. However, the boiling method produced more signals compared to the immersion method. Furthermore, results from the MRI images show that, of the specimens with a w/c ratio of 0.45, 0.55, and 0.65, the images obtained using the vacuum method were clearer than those obtained using the boiling method, and those obtained using the boiling method were clearer than those obtained using the immersion method. Therefore, we can reasonably infer that when specimens possess identical w/c ratios, the vacuum method is more effective for saturation compared to the boiling method, and the boiling method is more effective compared to the immersion method. In other words, of the three saturation methods, the immersion method achieves the least satisfactory saturation results.

The volume ratio of the bright zone in a specimen was defined as follows:

Table 3. MRI results using immersion method, boiling method, and vacuum method for various w/c ratios.

Result / Specimen	Volume of the specimen (cm^3)	Volume of bright zones obtained using MRI (cm^3)	Volume ratio of the bright zone
I1	1.7965	0.0407	0.0227
I2	1.7983	0.0472	0.0262
I3	1.7811	0.0538	0.0302
B1	1.7965	0.0415	0.0231
B2	1.7983	0.0483	0.0269
B3	1.7811	0.0571	0.0321
V1	1.7965	0.0517	0.0288
V2	1.7983	0.0596	0.0331
V3	1.7811	0.0735	0.0413

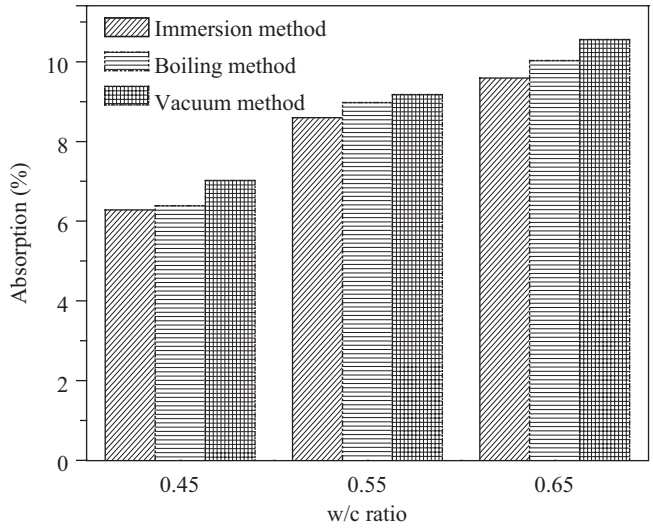

Fig. 5. Absorption results of various w/c ratios obtained using different methods.

$$\text{Volume ratio of bright zone} = \text{total bright zones volume/total volume of the specimen} \quad (2)$$

Here, the total bright zone volume, acquired from the relationship between the voxel (pixel axis x × pixel axis y × pixel axis z) and resolution refer to the colored sections in the MRI images. The total volume of the specimen was obtained using the Archimedes' principle.

The software used in this study was the Avizo 6.0 commercial image processing software. After the MRI results of specimens with w/c ratios of 0.65, 0.55, and 0.45 were inputted into the software, we determined the required bright zones and applied software tools to separate the required images from the unnecessary signals. The volume of the bright zones

Table 4. Compressive strength of specimens with w/c ratios of 0.65, 0.55, and 0.45.

Specimen	compressive strength (MPa)	average compressive strength (MPa)
w/c ratio = 0.65	38.36	38.34
	38.16	
	38.49	
w/c ratio = 0.55	43.84	43.79
	43.91	
	43.62	
w/c ratio = 0.45	55.78	55.47
	55.27	
	55.35	

Table 5. Comparisons of MRI images, and absorption techniques using different methods.

Data from various experiments / w/c	Volume ratio of the bright zone (immersion method)	volume ratio of the bright zone (boiling method)	volume ratio of the bright zone (vacuum method)	Absorption obtained using the immersion method (%)	Absorption obtained using the boiling method (%)	Absorption obtained using the vacuum method (%)
0.65	0.0302	0.0321	0.0413	9.59	10.03	10.56
0.55	0.0262	0.0269	0.0331	8.60	8.98	9.18
0.45	0.0227	0.0231	0.0288	6.28	6.39	7.02

was then calculated. The computation results were obtained using Avizo 6.0, as shown in Table 3. Based on these results, we can obtain the following conclusions:

According to the MRI image for a w/c ratio of 0.65 under conditions of the immersion method, the volume ratio of the bright zone calculated using Avizo 6.0 was 0.0302; this value is greater than that for the w/c ratio of 0.55. The volume ratio of the bright zone for the w/c ratio of 0.55 was 0.0262; this value is greater than that for the w/c ratio of 0.45, which obtained a value of 0.0227.

According to the MRI image for the w/c ratio of 0.65 under conditions of the boiling method, the volume ratio of the bright zone calculated using Avizo 6.0 was 0.0321; this value is greater than that for the w/c ratio of 0.55. The volume ratio of the bright zone for the w/c ratio of 0.55 was 0.0269; this value is greater than that for the w/c ratio of 0.45, which obtained a value of 0.0231.

According to the MRI image for the w/c ratio of 0.65 under conditions of the vacuum method, the volume ratio of the bright zone calculated using Avizo 6.0 was 0.0413; this value is greater than that for the w/c ratio of 0.55. The volume ratio of the bright zone for the w/c ratio of 0.55 was 0.0331; this value is greater than that for the w/c ratio of 0.45, which obtained a value of 0.0288.

The results show that for the three specimens with w/c ratios of 0.65, 0.55, and 0.45, an identical pattern emerges. That is, the volume ratio of the bright zone determined by MRI and computed by Avizo 6.0 under the vacuum method condition is greater than that under the boiling method condition. Additionally, the volume ratio of the bright zone under the boiling method condition is greater than that under the immersion method condition.

Regarding the specimen with the w/c ratio of 0.65, the number of bright zones calculated by Avizo 6.0 based on the MRI image under the vacuum method condition was 0.0735; this value is greater than that obtained under the boiling method condition. The number of bright zones under the boiling method condition was 0.0571; this value is greater than that obtained under the immersion method condition, which was 0.0538.

Regarding the specimen with the w/c ratio of 0.55, the number of bright zones calculated by Avizo 6.0 based on the MRI image under the vacuum method condition was 0.0596; this value is greater than that obtained under the boiling method condition. The number of bright zones under the boiling method condition was 0.0483; this value is greater than that obtained under the immersion method condition, which was 0.0472.

Regarding the specimen with a w/c ratio of 0.45, the number of bright zones calculated by Avizo 6.0 based on the MRI image under the vacuum method condition 0.0517; this value is greater than that obtained under the boiling method condition. The number of bright zones under the boiling method condition was 0.0415; this value is greater than that obtained under the immersion method condition, which was 0.0407. These results indicate that for the same specimen, the vacuum method provided the highest number of bright zones

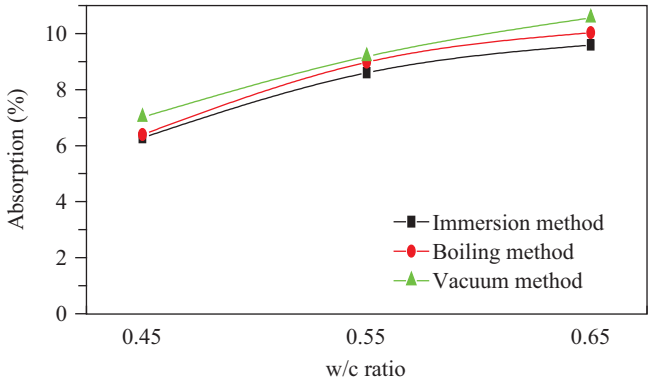

Fig. 6. Line chart of absorption of various w/c ratios obtained using different methods.

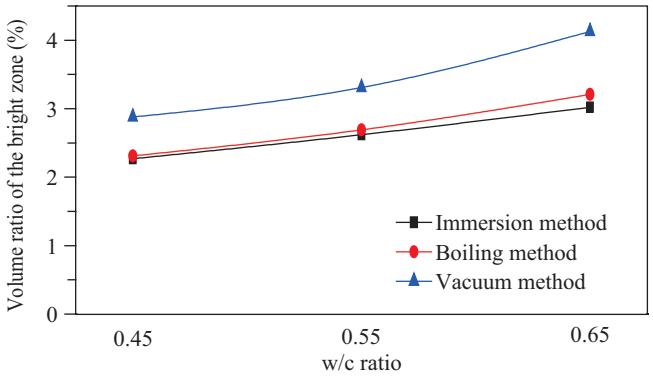

Fig. 7. Line chart of volume ratio of the bright zone of various w/c ratios using different methods.

in the MRI scan, the boiling method provided a moderate number of bright zones, and the immersion method provided the lowest number of bright zones. The vacuum method enabled the specimen to achieve the optimal moisture conditions for an MRI scan. By the way, the location of the bright zones is the site of water, which is also the location of the pores. We can reasonably conclude that the number of pores in the specimen for the w/c ratio of 0.65 is greater than that for the w/c ratio of 0.55. The number of pores in the specimen with a w/c ratio of 0.55 is greater than that of the w/c ratio of 0.45. Briefly, the results of this study show that a greater w/c ratio suggests a higher number of pores.

3. Standard Test Method for Compressive Strength of Mortars

The results shown in Table 4 indicate that the result for compressive strength, which was conducted on mortars with w/c ratios of 0.65, 0.55, and 0.45, respectively. The results shown in Tables 4 and 5 and Figs. 6 and 7 indicate that regardless of whether the immersion, boiling, or vacuum methods with w/c ratio conditions are employed, the volume ratio of the bright zone and the absorption are positively correlated. The high volume ratio of the specimen's bright zone denoted high porosity and high absorbency. Higher porosity meant lower relative strength. A higher w/c ratio indicates a higher water absorption rate; therefore, a higher w/c ratio suggests lower compressive strength, which leads to higher porosity.

V. CONCLUSIONS

The bright zone signals detected by MRI originate from the water in the pores of the mortars. A higher w/c ratio suggests a higher volume ratio for the bright zone. Additionally, the higher the number of bright zones, the higher the number of pores, whereas mortars with a low w/c ratio have a relatively low number of pores. Therefore, the greater the w/c ratio is, the more water it absorbs; however, the lower the compressive strength is. Additionally, the vacuum method provides the highest volume ratio of the bright zone under any w/c ratios. This indicates that the vacuum method can saturate the pores with water the easiest.

The absorption results and MRI images indicate that, considering the three methods for measuring the mortar saturation at different w/c ratios, the vacuum method is more effective than the boiling method, and the boiling method is more effective than the immersion method. Thus, water cannot completely saturate the dead-end pores in the immersion and boiling methods. The vacuum method tended to yield the most satisfactory mortar saturation results for MRI scanning.

ACKNOWLEDGMENTS

The authors wish to express their appreciation to the Preparatory Office of the Institute of Biomedical Sciences (IBMS) for providing the venue and MRI system required for the experiments.

REFERENCES

1. ASTM C109/C109M-11, "Standard test method for compressive strength of hydraulic cement mortars (using 2-in. or [50-mm] cube specimens)," American Society for Testing and Material (2011).
2. ASTM C642-06, "Standard test method for density, absorption, and voids in hardened concrete," American Society for Testing and Material (2006).
3. ASTM C1202-97, "Standard test method for electrical indication of concrete's ability to resist chloride ion penetration," American Society for Testing and Material (1997).
4. Beyea, S. D., Balcom, B. J., Mastikhin, I. V., Bremner, T. W., Armstrong, R. L., and Grattan-Bellew, P. E., "Imaging of heterogeneous materials with a turbo spin echo single-point imaging technique," *Journal of Magnetic Resonance*, Vol. 144, pp. 255-265 (2000).
5. Bushong, S. C., *Magnetic Resonance Imaging: Physical and Biological Principles*, 2nd Ed., Mosby-Year Book, St. Louis (1996).
6. Hornak, J. P., *The Basics of MRI*, Retrieved November 11, 2011 from http://www.cis.rit.edu/htbooks/mri/.
7. Huang, R., Chen, C. H., Cheng, A., and Xiu, H. J., "Experimental study of steel bar and concretes surface processing potency," Architecture and Building Research Institute, Ministry of the Interior (2004).
8. Jaffer, S. J., Lemaire, C., Hansson, C. M., and Peemoeller, H., "MRI: A complementary tool for imaging cement pastes," *Cement and Concrete Research*, Vol. 37, pp. 369-377 (2007).
9. Lane, D. S. and Ozyildirim, C., "Combinations of pozzolans and ground,

granulated, Blast-furnace slag for durable hydraulic cement concrete," Virginia Transportation Research Council (1999).
10. Safiuddin, Md. and Hearn, N., "Comparison of ASTM saturation techniques for measuring the permeable porosity of concrete," *Cement and Concrete Research*, Vol. 35, pp. 1008-1013 (2005).
11. Young, J. J., Szomolanyi, P., Bremner, T. W., and Balcom, B. J., "Magnetic resonance imaging of crack formation in hydrated cement paste materials," *Cement and Concrete Research*, Vol. 34, pp. 1459-1466 (2004).